Research Article Open Access

Piceatannol enhances contractile force in 3D engineered skeletal muscle tissues

Haruka Kimura, Naoko Matsui, Kaoru Ishihara, Ryouichi Ito, Shinpei Kawakami, Yukihiro Oritani and Naoki Iemoto

Morinaga & Co., Ltd., 2-1-1 Shimosueyoshi, Tsurumi-ku, Yokohama, 230-8504, Japan

***Corresponding author:** Naoko Matsui, Morinaga & Co., Ltd., 2-1-1 Shimosueyoshi, Tsurumi-ku, Yokohama, 230-8504, Japan, Email: n-matsui-ah@morinaga.co.jp

Editorial office: Editor@FFHDJ.com

Submission Date: February 4th, 2026; **Acceptance Date:** March 11th, 2026; **Publication Date:** March 19th, 2026

Please cite this article as: Kimura H., Matsui N., Ishihara K., Ito R., Kawakami S., Oritani Y., Iemoto N. Piceatannol enhances contractile force in 3D engineered skeletal muscle tissues. *Functional Foods in Health and Disease* 2026; 16(3): 268 – 280. DOI: https://doi.org/10.31989/ffhd.v16i3.1927

ABSTRACT

Background: Skeletal muscle underpins movement, metabolic homeostasis, and overall health. Age- and disease-related declines in muscle function lead to disability and increased healthcare burden. Piceatannol (PIC), a polyphenol abundant in passion fruit seeds, has shown antioxidant and metabolic effects in muscle cells. However, its direct impact on contractile force remains unclear. Three-dimensional (3D) engineered skeletal muscle provides a physiologically relevant *in vitro* model that enables direct measurement of contractile force.

Objective: We investigated the effects of PIC on contractile force in 3D engineered skeletal muscle and the underlying molecular pathways.

Methods: 3D engineered tissues were generated from C2C12 myoblasts embedded in type I collagen and differentiated in serum-reduced medium. Constructs were treated with 50 or 100 µM PIC or vehicle. Contractile force was measured at baseline (pre-treatment) and at weeks 1 and 2 post-treatment using electrical pulse stimulation, by tracking displacement of flexible pillars. RNA-seq was performed on two-dimensional (2D) cultured myotubes to identify genes differentially expressed following PIC treatment, and key findings were validated by RT-qPCR.

Results: PIC increased contractile force relative to vehicle in the 3D skeletal muscle tissues. At 50 µM, contractile force was significantly higher than vehicle at week 2; at 100 µM, it was significantly higher at both weeks 1 and 2. Transcriptomic analysis revealed enrichment of pathways related to carbohydrate metabolism, particularly glycolysis and glucose handling. RT-qPCR confirmed increased expression of *Glut4* and glycolytic enzymes, including *Hk2*, *Pfkm*, and *Pkm*.

Conclusion: In 3D engineered skeletal muscle, PIC enhanced contractile force and upregulated genes related to glucose uptake and glycolysis. These preclinical findings support and inform the development of PIC-containing functional foods aimed at preserving muscle function.

Novelty of the Study: This study is the first to demonstrate, in a physiologically relevant 3D engineered skeletal muscle model that overcomes 2D culture limitations, that PIC increases contractile force measured directly. It further implicates glycolytic activation as the underlying mechanism.

Keywords: muscle function; contractile force; skeletal muscle; glycolysis; piceatannol; polyphenol; 3D engineered skeletal muscle tissues

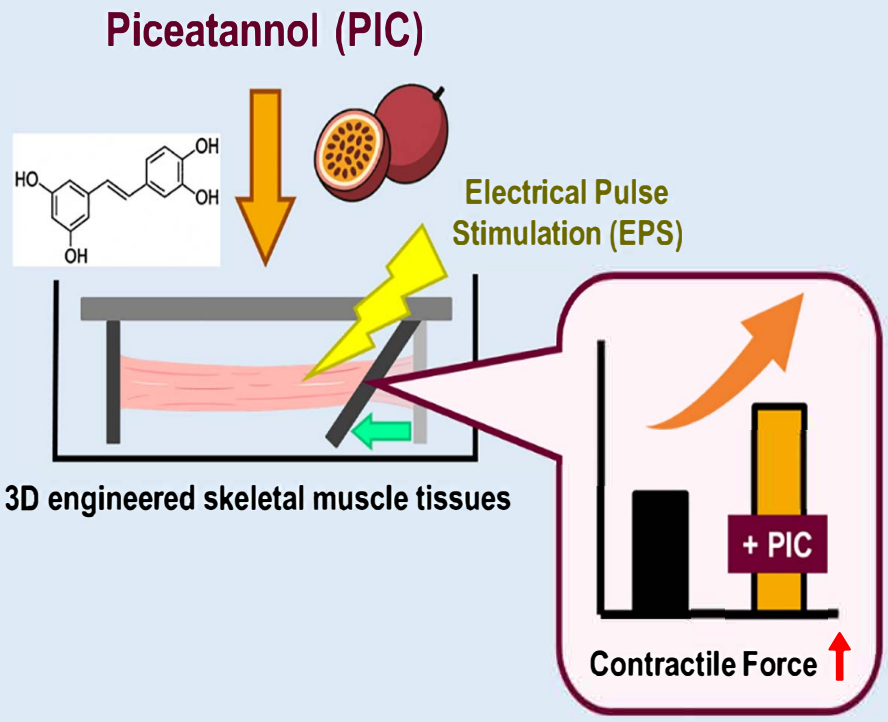

Graphical Abstract: PIC enhances contractile force in 3D engineered skeletal muscle tissues.

INTRODUCTION

Skeletal muscle constitutes approximately 45% of the total body mass and plays indispensable roles not only in maintaining motor function but also in respiration, metabolic regulation, and the homeostasis of the internal environment [1]. Muscle contraction is the most fundamental and critical function of skeletal muscle and is essential for limb movement, respiration, and metabolic control [2]. Impairment of muscle contractility and function due to aging, trauma, genetic factors, or diseases significantly impact quality of life and functional independence [2-3].

Sarcopenia is characterized by age-related decreases in skeletal muscle mass and strength and is closely associated with impaired mobility, loss of independence among older adults, increased risk of falls and fractures, and elevated mortality [3, 4]. Its prevalence is reported to be 5–13% in individuals aged 60–70 years and can reach up to 50% in those over 80 years [3, 5]. The development and progression of sarcopenia involve multiple factors, including aging, prolonged bed rest, physical inactivity, malnutrition, and chronic disease, as well as the combined effects of reduced physical activity, poor nutritional status, vitamin D deficiency, chronic inflammation, hormonal imbalance, and genetic predisposition [3-5].

Furthermore, abnormalities at the molecular and cellular levels—such as increased oxidative stress, mitochondrial dysfunction, and Ca^{2+} dysregulation—are major contributors to reduced muscle contractility [6, 7]. Sarcopenia-induced deficits in motor function, increased risk of falls and fractures, and the growing population requiring nursing care have resulted in greater medical and social burdens, including rising healthcare costs [4, 8]. Therefore, elucidating the pathophysiology and developing preventive and therapeutic strategies to maintain and improve contractile force remain critical research topics [7, 9].

For physiological and pathophysiological studies on skeletal muscles, as well as for the development of novel therapeutics, two-dimensional (2D) culture models have been widely employed [10-12]. However, 2D models have limitations, including their inability to recapitulate key skeletal muscle structures such as fiber alignment and sarcomere organization, making it difficult to evaluate physiological functions such as contractility [2, 13]. To overcome these shortcomings, three-dimensional (3D) engineered skeletal muscle tissues have recently gained attention as a promising technology [2, 10-11, 13, 14]. 3D culture models more accurately recapitulate *in vivo* muscle architecture and function and are also considered important alternatives to animal experimentation [10, 13]. Moreover, the development of 3D muscle tissues has enabled the establishment of assay systems for directly evaluating muscle contractile capacity [2, 11], and their applications have expanded to include the effects of food components and pharmaceuticals, such as quercetin [14-16]. Thus, 3D engineered skeletal muscle tissues compensate for the limitations of conventional models and are becoming a critical foundation for applications such as skeletal muscle research, disease mechanism elucidation, novel treatment development, and functional food evaluation.

Piceatannol (PIC), which has a stilbene structure [17], is a type of polyphenol abundantly present in passion fruit seeds [18] and exhibits various physiological activities, including antioxidant [19] and anti-inflammatory effects [20]. In skeletal muscles, PIC has been reported to alleviate oxidative stress [19] and increase glucose uptake by promoting glucose transporter type 4 (GLUT4) translocation [21]. In addition, recent studies have revealed that PIC upregulates the expression of sirtuin1 (SIRT1), a member of the sirtuin family of NAD^+-dependent deacetylases [22-24]. SIRT1 plays a key role in the regulation of energy metabolism, mitochondrial biogenesis, fatty acid

metabolism, maintenance of muscle fiber strength, and skeletal muscle recovery [22, 24]. Several studies have shown that PIC administration increases the expression of SIRT1 and mitochondrial function-related genes in skeletal muscle cells and contributes to the regulation of energy and lipid metabolism via SIRT1 [22, 24]. These findings suggest that the PIC-induced upregulation of SIRT1 expression in skeletal muscle may not only reduce oxidative stress and improve metabolic function but also help maintain skeletal muscle function. However, to date, no studies have directly investigated the effects of PIC on contractile force. Therefore, the aim of this study was to elucidate the effect of PIC on skeletal muscle contractile function using 3D cultured muscle tissue and to explore its underlying mechanisms.

METHODS

Cell Culture: C2C12 mouse skeletal muscle cells were obtained from the American Type Culture Collection (ATCC, Manassas, VA, USA). The myoblasts were cultured in growth medium (GM) consisting of high-glucose Dulbecco's Modified Eagle's Medium (DMEM; 4,500 mg/L glucose; Thermo Fisher Scientific, Tokyo, Japan) supplemented with 10% heat-inactivated fetal bovine serum (FBS; Cytiva, Logan, UT, USA), 1% Penicillin-Streptomycin-Glutamine (PSG; Thermo Fisher Scientific), and 1% Sodium Pyruvate (Thermo Fisher Scientific). Cells were incubated at 37°C in a 5% CO_2 environment. Once the cells achieved approximately 70% confluency, the GM was replaced with differentiation medium (DM) containing 2% heat-inactivated horse serum (HS; Thermo Fisher Scientific), hereafter referred to as 2% DM. This 2% DM, composed of high-glucose DMEM and 1% PSG, was refreshed every 2–3 days. After 4 days, the cells successfully differentiated into myotubes.

Fabrication of 3D Engineered Skeletal Muscle Tissues: 3D engineered skeletal muscle tissues were constructed using cultured C2C12 cells and a custom-made polydimethylsiloxane (PDMS) device, as previously described [13]. The PDMS device was placed at the center of a well in a 6-well plate. C2C12 cells were suspended in a type 1 collagen gel solution (Cellmatrix Type I-A; Nitta Gelatin, Osaka, Japan) at a density of 1.0×10^7 cells/mL. To prevent premature gelation, the mixture was mixed uniformly while cooling. A 100 µL aliquot of the cell-collagen mixture was then seeded onto the device and incubated at 37°C for 30 minutes to allow gel solidification. The cell-collagen mixture was cultured in GM for 2 days, after which the GM was replaced with DM containing 7% heat-inactivated HS (hereafter referred to as 7% DM), consisting of high-glucose DMEM and 1% PSG. The platform was inverted on the same day to facilitate observation under a microscope.

Compound Treatment for Cultured Models: PIC (Tokyo Chemical Industry Co., Ltd., Tokyo, Japan) was dissolved in dimethyl sulfoxide (DMSO; FUJIFILM Wako Pure Chemical Corporation, Osaka, Japan) and diluted to the desired concentration using DM. For the 2D culture model, the diluted PIC solution was prepared in 2% DM and applied to the myotubes. Myotubes were harvested at 10, 18, and 24 hours post-treatment. In the 3D culture model, the PIC solution was diluted in 7% DM and administered 1 week after the initiation of differentiation. The PIC concentrations in this study are widely used in *in vitro* studies. [21, 24, 25]

In all experimental setups, the final concentration of DMSO was maintained at 0.1%. The control group was treated with DM containing 0.1% DMSO. Treatment conditions were standardized across all experiments.

Measurement of Muscle Contractile Force with Electrical Pulse Stimulation (EPS): Contractile force was

assessed at 1, 2, and 3 weeks after the initiation of differentiation. Based on the mean contractile force values at the 1-week time point, groups were arranged to ensure comparable baseline values across experimental conditions. Force measurements were performed as described previously [14]. Briefly, the platform containing the 3D engineered skeletal muscle tissue was inverted to enable observation under an inverted microscope (IX73, Olympus, Tokyo, Japan). Carbon electrodes (C-Dish, IonOptix, Westwood, MA, USA) were placed on either side of each platform. Electric pulse stimulation (EPS) was delivered using a C-Pace EM stimulator (IonOptix) with the following parameters: 20 V, 30 Hz, 2 ms pulse width, for 5 seconds. Displacement of the PDMS micropillar tip was recorded and analyzed to calculate contractile force (μN). Force was calculated by multiplying the displacement of the pillar tip (μm) by a spring constant of 0.31, as described previously [14].

RNA Isolation: Total RNA was isolated from cells using the QIAshredder and RNeasy Mini Kits (QIAGEN, Hilden, Germany) following the manufacturer's protocols. Cell lysates were first homogenized with a QIAshredder to ensure thorough disruption, followed by RNA purification using the RNeasy Mini Kit.

RNA-seq Analysis: Library preparation and sequencing were performed as previously described [13], using a TruSeq Stranded mRNA Library Prep Kit (Illumina, San Diego, CA, USA) and a NovaSeq 6000 platform (Illumina) to generate single-end reads (10^1 bp). Normalized gene expression data (FPKM) and read counts were provided by the NGS core facility. Differentially expressed genes (DEGs) were defined as those exhibiting an absolute fold change ≥ 2 compared with the control group. Functional annotation and enrichment analyses of Gene Ontology (GO) biological processes and KEGG pathways were performed using DAVID (https://davidbioinformatics.nih.gov/home.jsp). Statistical significance was set at p-value < 0.05.

cDNA Synthesis and RT-qPCR: The extracted RNA (1 μg) was reverse-transcribed into cDNA using the High-Capacity cDNA Reverse Transcription Kit (Applied Biosystems, Foster City, CA, USA). Real-time polymerase chain reaction (PCR) was performed using the Light-Cycler 96 Real-Time PCR system (Roche Molecular Diagnostics, Basel, Switzerland) with KAPA SYBR FAST qPCR Master Mix (Kapa Biosystems, Cape Town, South Africa). PCR cycling conditions included an initial denaturation at 95°C for 10 minutes, followed by 45 cycles of 95°C for 10 seconds and 60°C for 25 seconds. Gene expression levels of specific mRNAs were normalized to *β-actin* mRNA levels. Primer sequences used for RT-qPCR- were as follows:

β-actin (fwd: 5'- CATCCGTAAAGACCTCTATG -3'; rev: 5'-ATGGAGCCACCGATCCACA -3'), *Glut4* (fwd: 5'-GCCCGGACCCTATACCCTAT -3'; rev: 5'-AGAGCCGATCTGCTGGAAAC -3'), *Hk2* (fwd: 5'-GTGTGCTCCGAGTAAGGGTG -3'; rev: 5'-CAGGCATTCGGCAATGTGG -3'), *Pkm* (fwd: 5'-CCATCTACCACTTGCAGCTATTC -3'; rev: 5'-CACTGCAGCACTTGAAGGA -3'), *Pfkm* (fwd: 5'-ATCACAGCCGAGGAGGCTAC -3'; rev: 5'-GGCGGCCCATCACTTCTAAC -3').

Statistical Analysis: All data are presented as mean ± standard deviation (SD). Statistical analyses were performed using Student's t-test for comparisons

between two groups. A p-value < 0.05 was considered statistically significant. All analyses were conducted using Microsoft Excel to ensure rigorous evaluation of the data.

RESULTS

PIC Enhances Muscle Contractile Force:

To investigate the effects of PIC on the contractile force of 3D engineered skeletal muscle tissues, we measured the contractile force, as shown in Figure 1. The PIC concentrations used in this study were first confirmed to be non-cytotoxic in conventional 2D cultures, and no apparent adverse changes in tissue morphology or translucency were observed in the 3D muscle constructs at these concentrations during the experimental period. The 50 µM PIC group showed a significant increase in contractile force compared to the control at 2 weeks after treatment (Figure 1A). Additionally, the 100 µM PIC group exhibited a significant enhancement of contractile force at both 1 and 2 weeks compared to the control group (Figure 1B), indicating that the improvement in contractile force was observed earlier at a higher concentration.

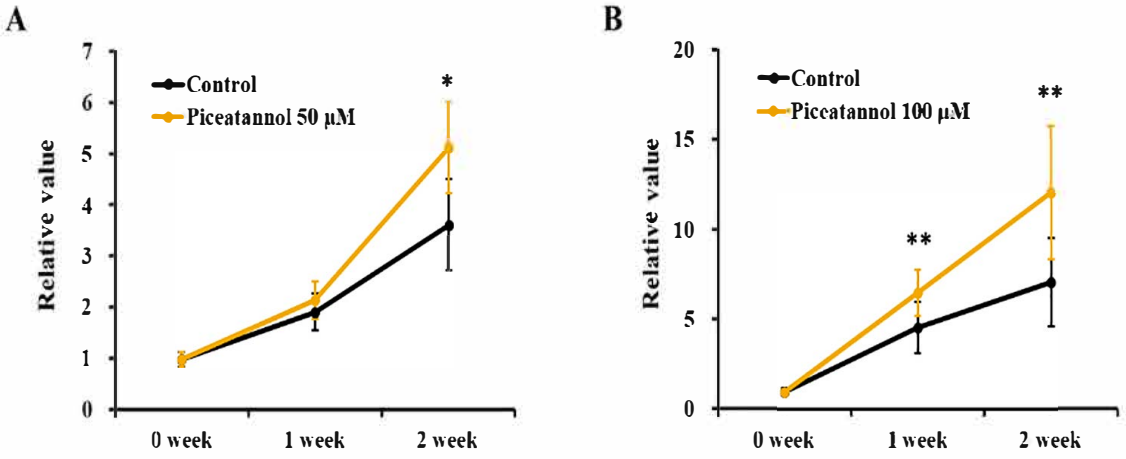

Figure 1. Effects of PIC on contractile force of 3D engineered skeletal muscle. Time course of contractile force in 3D engineered skeletal muscle treated with (A) 50 µM PIC or 0.1% DMSO (control) (n = 7), and (B) 100 µM PIC or 0.1% DMSO (control) (control: n = 9, PIC: n = 10), at 0, 1, and 2 weeks after treatment. Contractile force at each time point was normalized to its value at 0 week. Data are presented as mean ± SD. Statistical comparisons were performed between each PIC group and the respective control at each time point using Student's t-test. *p < 0.05, **p < 0.01.

PIC Activates Carbohydrate Metabolic Pathway: To elucidate the mechanisms underlying PIC-induced muscle strengthening, RNA-seq was performed using C2C12 myotubes cultured in 2D. As 100 µM PIC resulted in the most pronounced and rapid contractile force enhancement without detectable cytotoxicity, this concentration was selected for subsequent analyses. Samples were collected from the control (0.1% DMSO) and 100 µM PIC groups 10, 18, and 24 hours after treatment. Hierarchical clustering and Principal Component Analysis (PCA; iDEP2.0) showed a clear separation of gene expression profiles between groups and over time (Figure 2). For each gene, we calculated the fold change (FC) in expression between the PIC and control groups at 10, 18, and 24 hours. Genes for which |FC| was ≥ 2.0 at any of these time points and did not show a ≥ 2-fold change in the opposite direction at another time point were defined as DEGs. DEGs were

defined as genes showing a substantial and consistent change in expression at least once. A total of 3,277 genes were identified as DEGs, of which 1,319 were upregulated and 1,958 were downregulated by PIC. To reduce noise from lowly expressed genes in the enrichment analysis, we excluded genes with read counts below 10 in the control group at all time points (10, 18, and 24 hours). GO and KEGG analyses of the upregulated genes revealed enrichment of carbohydrate metabolism-related processes, especially glycolysis (Table 1, Table 2). In contrast, the TCA cycle and other downstream pathways were not significantly enriched. These findings suggest that PIC mainly activates genes involved in upstream carbohydrate metabolism.

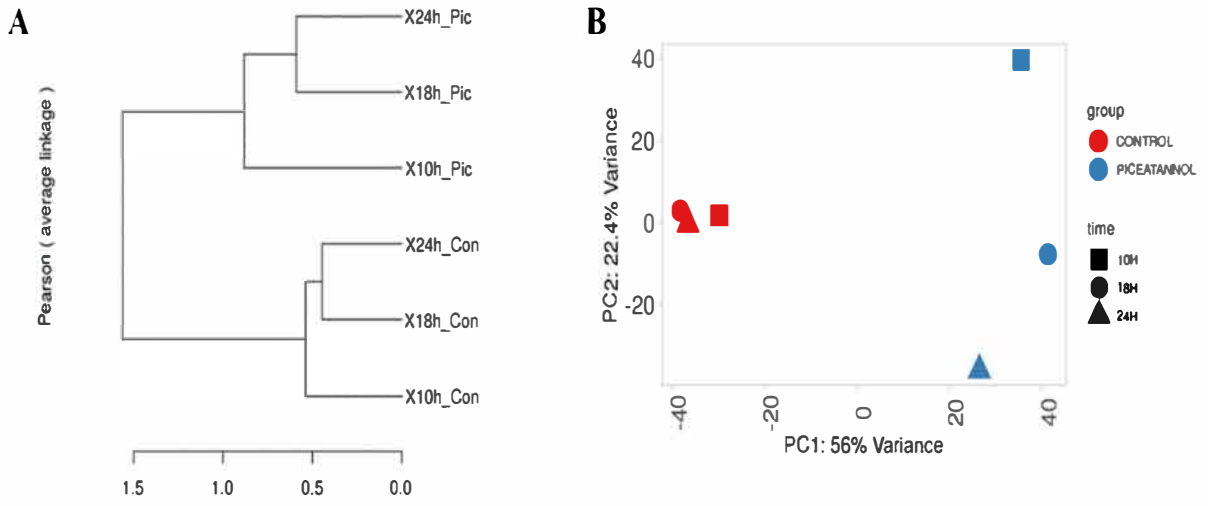

Figure 2. Transcriptomic analysis of PIC-treated C2C12 myotubes by RNA-seq. (A) Hierarchical clustering dendrogram of gene expression in C2C12 myotubes treated with 0.1% DMSO (control) or 100 μM PIC at 10, 18, or 24 hours. (B) PCA plot of the same samples showing transcriptomic variation by group and time (squares: 10 h; circles: 18 h; triangles: 24 h; red: control; blue: PIC). Samples were cultured in 2D and analyzed by RNA-seq (n = 1/condition). Analyses performed with iDEP2.0 (https://bioinformatics.sdstate.edu/idep/).

Table 1. GO enrichment analysis of DEGs in PIC-treated C2C12 myotubes

GO term (Biological Process)	GO ID	Count	*p*-value
glycolytic process	GO:0006096	8	2.14E-03
carbohydrate metabolic process	GO:0005975	12	4.35E-03
cellular response to glucose starvation	GO:0042149	8	8.09E-03
positive regulation of D-glucose import	GO:0046326	6	2.76E-02
fructose 1,6-bisphosphate metabolic process	GO:0030388	3	5.12E-02
regulation of glycolytic process	GO:0006110	3	9.39E-02

DEGs were defined as genes with ≥ 2-fold change between PIC and control (0.1% DMSO) at 10, 18, or 24 hours, excluding genes with control read count < 10. "Count" is the number of DEGs per GO term. Analysis was performed by DAVID (https://davidbioinformatics.nih.gov/home.jsp). Terms were selected by raw $p < 0.05$ or biological relevance.

Table 2. KEGG pathway enrichment analysis of DEGs in PIC-treated C2C12 myotubes.

KEGG pathway	KEGG ID	Count	*p*-value
Fructose and mannose metabolism	mmu00051	8	1.15E-03
Glycolysis / Gluconeogenesis	mmu00010	10	3.60E-03

DEGs were defined as ≥ 2-fold change between PIC and control at 10, 18, or 24 hours, excluding genes with control read count < 10. "Count" is the number of DEGs per pathway. Analysis was performed by DAVID. Pathways were selected by raw $p < 0.05$ or biological relevance. (https://davidbioinformatics.nih.gov/home.jsp)

Promotes Expression of Genes Involved in Carbohydrate Metabolism: Since the RNA-seq analysis was exploratory due to limitations such as small sample size, we validated its findings using RT-qPCR. C2C12 myotubes cultured in 2D were treated with PIC (100 μM) for 10 hours, after which gene expression was quantified by RT-qPCR. Expression levels of each gene were normalized to the endogenous control *β-actin* and expressed relative to the control group (0.1% DMSO). Based on RNA-seq and GO/KEGG pathway analyses indicating effects on genes involved in upstream stages of carbohydrate metabolism, we focused on *Glut4*, a key glucose transporter, and three glycolytic enzymes: hexokinase 2 (*Hk2*), phosphofructokinase (*Pfkm*), and pyruvate kinase (*Pkm*) for validation by RT-qPCR. The results showed that the PIC-treated group exhibited significant upregulation of *Glut4* as well as all three glycolytic enzymes (Figure 3). These findings suggest that PIC enhances upstream carbohydrate metabolic processes in C2C12 myotubes.

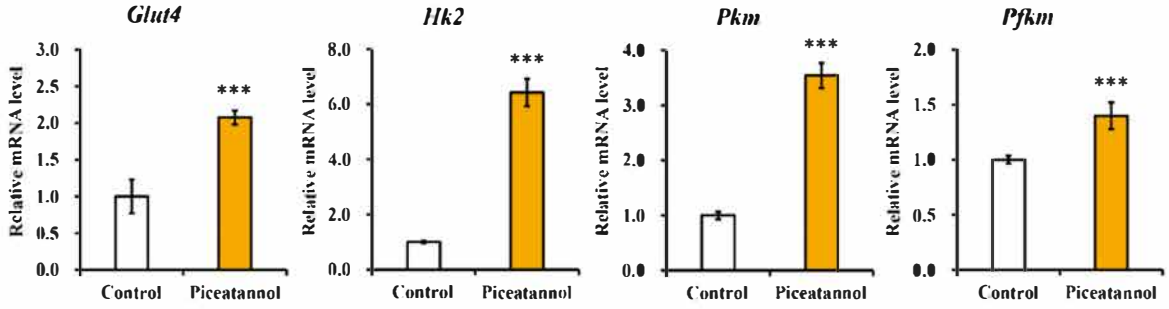

Figure 3. Effect of PIC on relative gene expression in C2C12 myotubes. C2C12 myotubes were treated with 100 μM PIC for 10 hours. Gene expression was normalized to *β-actin* and shown relative to control (0.1% DMSO). Data are mean ± SD (n = 4 per group). Statistical analysis by Student's *t*-test. ***$p < 0.001$.

DISCUSSION

In this study, using a 3D cultured muscle model with C2C12 cells, we demonstrated for the first time that PIC enhances contractile force. Previous studies utilizing conventional 2D culture systems have reported several effects of PIC on muscle cells, such as attenuation of oxidative stress [19], induction of SIRT1 expression [22], promotion of lipid metabolism, and enhancement of mitochondrial energy metabolism [24], highlighting a potential role of PIC in maintaining skeletal muscle function. However, 2D culture systems arrange myocytes in a monolayer on a flat substrate, which fails to recapitulate the maturation, complex alignment, and 3D architecture observed *in vivo* in muscle tissues [2, 13]. Consequently, direct measurement of contractile force is challenging in 2D cultures, and the actual impact of PIC

on muscle contractility remains unclear. The 3D cultured muscle model employed in the present study enabled a more direct evaluation of skeletal muscle contractility compared to 2D systems [10], enabling us to clarify the contractile force-enhancing effects of PIC. This finding suggests the potential application of PIC in preventing or ameliorating age-related muscle decline, such as sarcopenia, and supports its utility as a functional food ingredient or health-promoting compound to maintain or improve skeletal muscle function.

RNA-seq combined with GO/KEGG analysis revealed that genes associated with carbohydrate metabolism, particularly glycolysis and carbohydrate metabolic processes, were upregulated in the PIC-treated group. Notably, this included the glucose transporter GLUT4 and the key glycolytic enzymes hexokinase (HK), phosphofructokinase (PFK), and pyruvate kinase (PK). GLUT4 is the primary insulin-responsive glucose transporter and plays a critical role in mediating glucose uptake in skeletal muscle cells [26]. HK, PFK, and PK are central regulators of glycolysis, serving as rate-limiting or flow-controlling enzymes essential for metabolic regulation [27]. Previous studies have shown that PIC activates the AMPK pathway in muscle cells and enhances glucose uptake by promoting GLUT4 translocation to the cell membrane [21]. The activity of GLUT4 in skeletal muscle is primarily governed by its translocation [28].

Consistent with these findings, the present study demonstrated upregulation of GLUT4, suggesting that PIC enhances glucose transport in skeletal muscle cells by both increasing GLUT4 expression and facilitating its translocation, processes that collectively improve glucose utilization. Moreover, earlier studies have reported PIC-induced increases in ATP production [24], providing important evidence that upregulation of glycolysis-related genes observed in the present study enhances the cellular energy production capacity. Notably, accelerated glycolysis increases ATP availability, which rapidly supplies energy to muscle tissue [29], and a sufficient ATP supply is known to directly enhance muscle strength [30]. Collectively, these results suggest that the PIC-mediated promotion of glucose metabolism and the resulting increase in ATP production may reinforce the energy supply required for muscle contraction, ultimately enhancing contractile force.

Generally, increased muscle strength is determined by muscle cross-sectional area [31], quantity and function of contractile proteins [32], and neurological adaptations [33]. However, in this study, no apparent increase in myotube diameter or upregulation of contraction-related genes was observed. Furthermore, we used a muscle cell-only culture model without neurons, as EPS-induced contractions operate via mechanisms distinct from neurotransmission *in vivo* [34, 35]. Thus, phenomena from nervous system or neuromuscular interactions could not be assessed. Overall, the observed rise in contractile force is likely due to elevated ATP production via metabolic activation, as discussed above.

This study has some limitations. First, the concentrations of PIC used in this study are widely used *in vitro* and were selected based on the absence of cytotoxicity; however, whether comparable levels are achieved *in vivo*, particularly in skeletal muscle tissue, remains unclear and warrants further investigation. Second, we used C2C12 cells, a mouse-derived skeletal muscle cell line; therefore, studies using human muscle cells or other muscle cell types may provide additional insights. Furthermore, regarding mitochondria-related pathways, such as the TCA cycle and oxidative phosphorylation, no notable changes were detected under the current experimental conditions. However, variations in cell type or experimental parameters (e.g., stimulation duration) may yield different results. Additionally, RNA-seq was conducted under 2D culture

conditions; thus, gene expression dynamics in 3D muscle tissue models may differ. Moreover, although neuronal systems are well known to play a crucial role in muscle strength regulation and adaptation, the current model lacked neuronal elements, precluding direct evaluation of neuromuscular interactions or neuronal adaptations. Therefore, future studies incorporating co-cultures with neuronal cells or neuromuscular complex models are warranted to elucidate the role of the nervous system in PIC-induced effects. Furthermore, since our investigation was primarily limited to molecular mechanism analysis, future research should encompass multifaceted functional assessments, such as fiber type-specific responses, mitochondrial function, lipid metabolism interactions, myogenic differentiation pathways, and evaluation of long-term effects. Moreover, the precise molecular targets of PIC remain unclear and require further investigation.

Previous studies have shown antioxidant and mitochondrial effects of PIC, whereas our work uniquely demonstrates its impact on "increased contractile force." It is essential to gather further evidence for the capacity of PIC to improve skeletal muscle function through experiments using more physiologically relevant *in vitro* models (e.g., 3D cultures), human muscle cells, disease and aging models, and *in vivo* systems. This study on muscle function remains at the preclinical study based on *in vitro* data. Therefore, additional studies in clinical trials are needed to establish the effects of PIC on muscle strength [36].

Scientific Innovation and Practical Implications: This research provides novel insights into PIC's capacity to enhance skeletal muscle function, demonstrating increased contractile force in 3D engineered muscle model. By coupling direct force measurements with metabolic profiling, it implicates glycolytic activation as a key mechanism. These findings support development of muscle-supportive nutrition and formulations and prompt further research and application.

CONCLUSION

PIC, abundant in passion fruit seeds, increased contractile force in a 3D engineered muscle model. Promotion of carbohydrate metabolism was suggested as a contributing factor to this enhancement. Taken together, these findings support the potential of PIC as a functional ingredient for supporting muscle function and warrant further investigation in advanced *in vitro* systems and translational studies.

List of Abbreviations: PIC: piceatannol, SIRT1: sirtuin1, 3D: three-dimensional, 2D: two-dimensional, DMSO: dimethyl sulfoxide, RT-qPCR: reverse transcription quantitative polymerase chain reaction, GM: growth medium, DM: differentiation medium, DMEM: Dulbecco's Modified Eagle's Medium, FBS: fetal bovine serum, HS: horse serum, PSG: penicillin-streptomycin-glutamine, EPS: electrical pulse stimulation, PDMS: polydimethylsiloxane, DEGs: differentially expressed genes, GO: gene ontology, PCA: principal component analysis, FC: fold change, ATP: adenosine triphosphate, AMPK: AMP-activated protein kinase, GLUT4: Glucose Transporter type 4, HK: Hexokinase, PFK: Phosphofructokinase, PK: Pyruvate kinase.

Authors' Contributions: Conceptualization, H.K., N.M., S.K., and Y.O; methodology, H.K., N.M., K.I., R.I., S.K., and Y.O.; original draft preparation, H.K.; writing—review and editing, N.M., S.K., and Y.O.; visualization, H.K.; supervision, N.I.; project administration, Y.O.

Competing interests: All authors are employees of Morinaga & Co., Ltd.

Acknowledgments and Funding: We are grateful to Drs. Tomohiro Nakamura, Sho Yokoyama and Toshiya Fujisato of Osaka Institute of Technology for their kind provision

of the device for 3D engineered skeletal muscle tissue construction and valuable guidance regarding the methodology. We also thank Drs. Takeshi Nikawa and Takayuki Uchida of Tokushima University for their insightful comments and suggestions regarding this work. Additionally, we acknowledge the NGS core facility at the Research Institute for Microbial Diseases of Osaka University for RNA sequencing and data analysis. This study was supported by Morinaga & Co., Ltd. This study received no external funding.

REFERENCES

1. Gao L., Li L., Wu W., Feng J., Liu Z., He J., et. al. 3d bio-printed in vitro skeletal muscle with pennate fibers architecture to enhance contractile function. International Journal of Bioprinting 2024; 10(6): 4371. DOI: https://doi.org/10.36922/ijb.4371.
2. Vesga-Castro C., Aldazabal J., Vallejo-Illarramendi A. and Paredes J. Contractile force assessment methods for in vitro skeletal muscle tissues. eLife 2022; 11. DOI: https://doi.org/10.7554/eLife.77204.
3. Liu D., Wang S., Liu S., Wang Q., Che X. and Wu G. Frontiers in sarcopenia: Advancements in diagnostics, molecular mechanisms, and therapeutic strategies. Molecular Aspects of Medicine 2024; 97: 101270. DOI: https://doi.org/10.1016/j.mam.2024.101270.
4. Dolan E., Artioli G.G., Pereira R.M.R. and Gualano B. Muscular atrophy and sarcopenia in the elderly: Is there a role for creatine supplementation? Biomolecules 2019; 9(11): 642. DOI: https://doi.org/10.3390/biom9110642.
5. Alizadeh Pahlavani H., Laher I., Knechtle B. and Zouhal H. Exercise and mitochondrial mechanisms in patients with sarcopenia. Frontiers in Physiology 2022; 13. DOI: https://doi.org/10.3389/fphys.2022.1040381.
6. Ahn B., Ranjit R., Kneis P., Xu H., Piekarz K.M., Freeman W.M., et al. Scavenging mitochondrial hydrogen peroxide by peroxiredoxin 3 overexpression attenuates contractile dysfunction and muscle atrophy in a murine model of accelerated sarcopenia. Aging Cell 2022; 21(3): e13569. DOI: https://doi.org/10.1111/acel.13569.
7. Murphy K.T., Ham D.J., Church J.E., Naim T., Trieu J., Williams D.A., et al. Parvalbumin gene transfer impairs skeletal muscle contractility in old mice. Human Gene Therapy 2012; 23(8): 824-836. DOI: https://doi.org/10.1089/hum.2011.210.
8. Buford T.W., Anton S.D., Judge A.R., Marzetti E., Wohlgemuth S.E., Carter C.S., et al. Models of accelerated sarcopenia: Critical pieces for solving the puzzle of age-related muscle atrophy. Ageing Res Rev 2010; 9(4): 369-383. DOI: https://doi.org/10.1016/j.arr.2010.04.004.
9. Larsson L., Degens H., Li M., Salviati L., Lee Y.I., Thompson W., et al. Sarcopenia: Aging-related loss of muscle mass and function. Physiological Reviews 2019; 99(1): 427-511. DOI: https://doi.org/10.1152/physrev.00061.2017.
10. Wang J., Khodabukus A., Rao L., Vandusen K., Abutaleb N. and Bursac N. Engineered skeletal muscles for disease modeling and drug discovery. Biomaterials 2019; 221: 119416. DOI: https://doi.org/10.1016/j.biomaterials.2019.119416.
11. Cao T. and Warren C.R. From 2d myotube cultures to 3d engineered skeletal muscle constructs: A comprehensive review of in vitro skeletal muscle models and disease modeling applications. Cells 2025; 14(12): 882. DOI: https://doi.org/10.3390/cells14120882.
12. Miura K., Hasumura M., Kitahara Y., Nishitani S. and Yamada Y. A novel amino acid mixture containing isoleucine, glycine, and cystine improves insulin sensitivity with restoring mitochondrial oxygen consumption in c2c12 myotubes. Functional Foods in Health and Disease 2025; 15(4): 205-216. DOI: https://doi.org/10.31989/ffhd.v15i4.1582.
13. Tollitt B.R., Jones S.W., Ohana J., Henstock J.R., Jackson M.J., et. al. comparison of human skeletal muscle cell maturation in 2d versus 3d culture: A quantitative proteomic study. Physiological Reports 2025; 13(12). DOI: https://doi.org/10.14814/phy2.70420.
14. Kishishita K., Nakamura T., Mizutani M., Fujisato T., Hashimoto T., Matsui N., et al. Novel platform for quantitative evaluation of medicinal efficacy based on contractility of artificial skeletal muscle. Journal of Biomechanical Science and Engineering 2023; 18(4): 23-00396-00323-00396. DOI: https://doi.org/10.1299/jbse.23-00396.

15. Yi D., Sugimoto T., Matsumura T., Yokoyama S., Fujisato T., Nakamura T. and Hashimoto T. Investigating the combined effects of mechanical stress and nutrition on muscle hypertrophic signals using contractile 3d-engineered muscle (3d-em). Nutrients 2023; 15(18). DOI: https://doi.org/10.3390/nu15184083.
16. Nagai A., Kaneda Y., Izumo T., Nakao Y., Honda H. and Shimizu K. Quercetin induces a slow myofiber phenotype in engineered human skeletal muscle tissues. FASEB Journal 2024; 38(16): e70009. DOI: https://doi.org/10.1096/fj.202400914RR.
17. Kawakami S., Morinaga M., Tsukamoto-Sen S., Mori S., Matsui Y. and Kawama T. Constituent characteristics and functional properties of passion fruit seed extract. Life (Basel) 2021; 12(1). DOI: https://doi.org/10.3390/life12010038.
18. Matsui Y., Sugiyama K., Kamei M., Takahashi T., Suzuki T., Katagata Y., et. al. Extract of passion fruit (passiflora edulis) seed containing high amounts of piceatannol inhibits melanogenesis and promotes collagen synthesis. Journal of Agricultural and Food Chemistry 2010; 58(20): 11112-11118. DOI: https://doi.org/10.1021/jf102650d.
19. Nonaka S., Kawakami S., Maruki-Uchida H., Mori S. and Morita M. Piceatannol markedly upregulates heme oxygenase-1 expression and alleviates oxidative stress in skeletal muscle cells. Biochemistry and Biophysics Reports 2019; 18. DOI: https://doi.org/10.1016/j.bbrep.2019.100643.
20. Ashikawa K., Majumdar S., Banerjee S., Bharti A.C., Shishodia S. and Aggarwal B.B. Piceatannol inhibits tnf-induced nf-kappab activation and nf-kappab-mediated gene expression through suppression of ikappabalpha kinase and p65 phosphorylation. Journal of Immunology 2002; 169(11): 6490-6497. DOI: https://doi.org/10.4049/jimmunol.169.11.6490.
21. Minakawa M., Miura Y. and Yagasaki K. Piceatannol, a resveratrol derivative, promotes glucose uptake through glucose transporter 4 translocation to plasma membrane in l6 myocytes and suppresses blood glucose levels in type 2 diabetic model db/db mice. Biochemical and Biophysical Research Communications 2012; 422(3): 469-475. DOI: https://doi.org/10.1016/j.bbrc.2012.05.017.
22. Tanaka K., Kawakami S., Mori S., Yamaguchi T., Saito E., Setoguchi Y., et al. Piceatannol upregulates sirt1 expression in skeletal muscle cells and in human whole blood: In vitro assay and a randomized, double-blind, placebo-controlled, parallel-group comparison trial. Life 2024; 14(5). DOI: https://doi.org/10.3390/life14050589.
23. Yoshihara M., Kawakami S., Matsui Y. and Kawama T. Piceatannol enhances hyaluronic acid synthesis through sirt1-mediated has2 upregulation in human dermal fibroblasts. Biochemistry and Biophysics Reports 2024; 39: 101746. DOI: https://doi.org/10.1016/j.bbrep.2024.101746.
24. Tsuda H., Uchida T., Okuno S., Ulla A., Kawakami S., Mori S., et al. Piceatannol enhances intracellular energy metabolism via sirt1 in c2c12 cells. Advances in Biological Chemistry 2025; 15(03): 54-69. DOI: https://doi.org/10.4236/abc.2025.153005.
25. Yamamoto T., Iwami S., Aoyama S., Maruki-Uchida H., Mori S., Hirooka R., et al. Effect of piceatannol on circadian per2 expression in vitro and in vivo. Journal of Functional Foods 2019; 56: 49-56. DOI: https://doi.org/10.1016/j.jff.2019.02.042.
26. Wang T., Wang J., Hu X., Huang X.J. and Chen G.X. Current understanding of glucose transporter 4 expression and functional mechanisms. World Journal of Biological Chemistry 2020; 11(3): 76-98. DOI: https://doi.org/10.4331/wjbc.v11.i3.76.
27. Zuo J., Tang J., Lu M., Zhou Z., Li Y., Tian H., et al. Glycolysis rate-limiting enzymes: Novel potential regulators of rheumatoid arthritis pathogenesis. Frontiers in Immunology 2021; 12: 779787. DOI: https://doi.org/10.3389/fimmu.2021.779787.
28. Richter E.A. and Hargreaves M. Exercise, glut4, and skeletal muscle glucose uptake. Physiological Reviews 2013; 93(3): 993-1017. DOI: https://doi.org/10.1152/physrev.00038.2012.
29. Koh J.H., Pataky M.W., Dasari S., Klaus K.A., Vuckovic I., Ruegsegger G.N., et al. Enhancement of anaerobic glycolysis - a role of pgc-1α4 in resistance exercise. Nat Commun 2022; 13(1): 2324. DOI: https://doi.org/10.1038/s41467-022-30056-6.
30. Cooke R. and Bialek W. Contraction of glycerinated muscle fibers as a function of the atp concentration. Biophysical Journal 1979; 28(2): 241-258. DOI: https://doi.org/10.1016/s0006-3495(79)85174-7.
31. Maughan R.J., Watson J.S. and Weir J. Strength and cross-sectional area of human skeletal muscle. Journal of Physiology 1983; 338: 37-49. DOI: https://doi.org/10.1113/jphysiol.1983.sp014658.
32. Thompson L.V., Durand D., Fugere N.A. and Ferrington

D.A. Myosin and actin expression and oxidation in aging muscle. J Appl Physiol (1985) 2006; 101(6): 1581-1587. DOI: https://doi.org/10.1152/japplphysiol.00426.2006.

33. Taube W. "What trains together, gains together": Strength training strengthens not only muscles but also neural networks. J Appl Physiol (1985) 2011; 111(2): 347-348. DOI: https://doi.org/10.1152/japplphysiol.00688.2011.
34. Cairns S.P., Chin E.R. and Renaud J.M. Stimulation pulse characteristics and electrode configuration determine site of excitation in isolated mammalian skeletal muscle: Implications for fatigue. J Appl Physiol (1985) 2007; 103(1): 359-368. DOI: https://doi.org/10.1152/japplphysiol.01267.2006.
35. Ito A., Yamamoto Y., Sato M., Ikeda K., Yamamoto M., Fujita H., et al. Induction of functional tissue-engineered skeletal muscle constructs by defined electrical stimulation. Scientific Reports 2014; 4: 4781. DOI: https://doi.org/10.1038/srep04781.
36. Martirosyan D. Functional food science in the era of artificial intelligence: The role of domain authority, structured validation, and responsible translation. Functional Food Science - Online ISSN: 2767-3146 2026; 6(2): 76-86. DOI: https://doi.org/10.31989/ffs.v6i2.1903.